Nematic ordering in a cell with modulated surface anchoring: Effects of flexoelectricity

G. Barbero,[1] G. Skačej,[2] A. L. Alexe-Ionescu,[3] and S. Žumer[2]
[1]*Dipartimento di Fisica del Politecnico di Torino and Istituto Nazionale di Fisica della Materia, Corso Duca degli Abruzzi 24, I-10129 Torino, Italy*
[2]*Physics Department, University of Ljubljana, Jadranska 19, SI-1000 Ljubljana, Slovenia*
[3]*Departamentul de Fizica, Universitatea Politehnica din Bucureşti, Splaiul Independentei 313, R-77206 Bucharest, Romania*
(Received 14 January 1999)

We have analyzed molecular ordering in a nematic sample sandwiched between two parallel substrates, characterized by a periodically varying anchoring easy axis. If the periodicity λ is smaller than the Debye screening length l_D and the nematic material possesses flexoelectric properties, it is necessary to take into account also the electrostatic and flexoelectric contributions in the thermodynamical potential when the actual director field is determined. In this framework, for small deviations from the homeotropic alignment we have derived analytical expressions for the tilt angle (θ) and the electrical potential. To establish a connection with experimentally observable quantities, we have related the θ profile to the average $\langle \theta^2 \rangle$ and investigated its behavior for different values of λ, the flexoelectric coefficient, and the anchoring strength w. Our results indicate that in a nematic with pronounced flexoelectric properties for small enough λ, a kind of subsurface deformation appears, which substantially decreases $\langle \theta^2 \rangle$. Therefore, effects of flexoelectricity cannot be neglected in treating nematic cells with modulated anchoring which allows bistable ordering.
[S1063-651X(99)07807-1]

PACS number(s): 61.30.−v

I. INTRODUCTION

Thermotropic nematic liquid crystals (NLCs) are organic materials formed by asymmetric (cigar or disklike) molecules. Sterical constraints originating from the shape anisotropy yield positive uniaxial optical properties [1]. Their optical axis coincides with the average molecular orientation, the nematic director **n**. Molecules forming nematic phases have, usually, net permanent electric dipolar and quadrupolar moments. However, due to molecular spinning and tumbling, any macroscopic polarization in an undistorted NLC on the average cancels out. This no longer holds if the NLC is deformed. In such a case it can manifest a flexoelectric polarization, connected with the spatial variation of the director **n**, defined by $P_i = \lambda_{ijk} \partial n_j / \partial x_k$. The tensor with elements λ_{ijk} is called flexoelectric tensor [1,2]. As discussed in [2], the flexoelectric polarization **P** can be written in the covariant form as $\mathbf{P} = e_{11}\mathbf{n}\,\mathrm{div}\mathbf{n} - e_{33}\mathbf{n}\times\mathrm{rot}\,\mathbf{n}$, where e_{11} and e_{33} are the flexoelectric coefficients. This polarization is similar to the piezoelectric polarization present in solid materials possessing no center of symmetry [3]. The flexoelectric polarization can have a dipolar [2] or quadrupolar [4] origin. The dipolar flexoelectricity is present when the molecules of the mesophase, in addition to the permanent electrical dipole, also possess shape anisotropy (pear or banana shape). In this case, a deformation of the director field can lead to a polarization of the medium. The quadrupolar origin of flexoelectricity is simpler to understand. In fact, a molecule can possess an electrical quadrupolar moment q_0, even if it does not have any shape anisotropy. The macroscopic density of the quadrupolar tensor can be written as $\mathcal{D}_{ij} = \rho q_0 \mathcal{Q}_{ij}$, where ρ is the particle density and $\mathcal{Q}_{ij}$ the tensor order parameter. It is defined by $\mathcal{Q}_{ij} = S[n_i n_j - (1/3)\delta_{ij}]$, where S is the NLC scalar order parameter [1]. If $\mathcal{D}_{ij}$ is not constant across the NLC sample, a net macroscopic polarization appears and is given by [5] $P_i = -\partial \mathcal{D}_{ij} / \partial x_j$, as it is well known from elementary electrostatics. Hence **P** can occur if there is either a variation of the director **n** (flexoelectricity [2]) or of the scalar order parameter S (order electricity [6]). This polarization is associated with long-range electrostatic interactions, which have to be taken into account in the thermodynamical potential, in addition to short-range interactions giving rise to the nematic phase.

The electric polarization caused by director deformations induces an electric field, which couples with the flexoelectric polarization itself [7]. The resulting electrostatic energy has to be taken into account when the nematic director field is determined [8]. In a case in which only one-dimensional problems are considered, a simple analysis shows that the electrostatic energy due to the flexoelectric polarization renormalizes the elastic anisotropy of the Frank elastic constants, with a term depending on the director orientation [9]. Long ago [10], it has been shown that taking into account the flexoelectric contribution to the total energy density, it is possible to explain apparent deviations from the surface energy proposed by Rapini and Papoular [11]. For a usual NLC cell where the sample of slab shape exhibits just a relatively weak one-dimensional deformation, the electrostatic energy density of flexoelectric origin can be neglected. In fact, commercial NLCs are characterized by a Debye screening length below one micron [12] so that in a cell where the deformation spreads over several micrometers the flexoelectric effect is screened by the ions present in the mesophase. In this framework, just a linear coupling of the flexoelectric polarization with an external field can be observed [13], but in the absence of an external field flexoelectric properties are not detectable. Of course the situation is completely different if one is interested in analyzing deformations taking place on distances small with respect to the Debye screening length. In this case the balance of mechanical torques and electrical

torques connected to the flexoelectric polarization requires to solve electrostatic and elastic problems to find the equilibrium director field [14].

Our interest in this problem is not only academic. In fact, it is well known that one of the techniques used to orient the NLC is based on SiO evaporation on glass substrates [15]. In such a case the surface topography is characterized by a periodicity which can be small with respect to the Debye screening length. Consequently, the NLC in contact with such substrates undergoes an elastic deformation whose characteristic length is also smaller than the Debye length, and therefore effects of flexoelectricity can become important. Another technique is based on constructing periodic micrometric surface structures (bigrating made with photosensitive materials) [16]. Also in this case, the surface periodicity can be well below the Debye screening length. Simple elastic models proposed to connect such surface geometry with the anisotropic part of the anchoring energy are just an extension of the Berreman–de Gennes model [1,17,18], in which the NLC energy density reduces to the Frank elastic energy density, thereby ignoring flexoelectricity. Similar studies concerning the bistability of nematic samples oriented by periodic sawtoothed surfaces have also been published [16,19,20]. The same model was used to measure the azimuthal anchoring energy on sinusoidal holographic unidimensional and bidimensional gratings [21]. However, for surface structures characterized by the submicrometric length scale, the Frank energy density represents only a very rough approximation of the total energy density. Therefore, in the past some attempts have been made to take into account also the flexoelectric contribution to the free energy in the Berreman–de Gennes model [22,23]. However, the main goal of these investigations was to evaluate the flexoelectricity-induced renormalization of the elastic constant.

So far we have reviewed only analyses in which the nematic state was completely characterized by the director **n**, which was equivalent to assuming that the NLC scalar order parameter S is constant across the nematic sample. A more realistic theoretical analysis has to take into account that both **n** and S are position-dependent. Within the Landau–de Gennes approach it is possible to show that surface induced spatial variations of S induce subsurface deformations in **n** [24]. Our analysis in Ref. [24] reports a simple one-dimensional problem where the spatial variation of S can be easily taken into account by the introduction of a quasi-splay-bend elastic constant. Similar results have been obtained by Vertogen's group [25]. The use of the Landau–de Gennes theory has been demonstrated in a study of orientational states induced in a NLC by microtextured substrates [26–28]. It has been shown [26,27] that spatially mixed patterns of different aligning potentials on a mesoscopic scale induce bulk orientational states which are temperature dependent. The analyses reported in [24–28] are all neglecting the possibility of deformation-induced polarization. However, $\mathcal{Q}_{ij}=\mathcal{Q}_{ij}(\mathbf{r})$ can lead to a macroscopic polarization, as discussed above, which can be either of flexoelectric or order electric origin.

The influence of the order electric polarization on the orientation of the liquid crystal at the surface was also discussed long ago in Ref. [6]. It was shown that the electrostatic energy due to the order electric polarization, in a simple one-dimensional geometry, can explain the tilted orientations observed experimentally at the nematic-isotropic interface [29]. A molecular theory of the order electricity has been proposed by Osipov and Sluckin [30]. These authors show that a Landau–de Gennes gradient expansion in the tensor order parameter has to be employed with extreme caution in an inhomogeneous NLC exhibiting flexoelectric and order electric effects.

The aim of the present paper is to show that the flexoelectric polarization can play a rather important role in determining the actual nematic director orientation in nematic structures with at least two-dimensional variation of the director field, similar to those considered for technological applications [15,16]. We will, however, neglect variations of the scalar order parameter S across the NLC sample and, consequently, effects of order electricity since the nematic correlation length associated to S variations is smaller than the typical deformation scales considered here [24]. We show that it is impossible to take into account the flexoelectric contribution to the thermodynamical potential density by simply renormalizing the elastic constants or the anisotropic part of the surface energy. To correctly take into account the flexoelectric polarization, it is necessary to solve a coupled elastic-electrostatic problem [14]. We limit our analysis to a simple case where the substrates in the NLC sample induce an orientation close to homeotropic. Moreover, using the one elastic constant approximation we assume, for simplicity, the splay and bend constants to be equal ($k_{11}=k_{33}=k$), and, again for the same reason, also the dielectric constant of the nematic material to be isotropic (i.e., $\epsilon_{||}=\epsilon_{\perp}=\epsilon$). Of course, the analysis can be easily modified to take into account the elastic and dielectric anisotropies, as well as the spatial variation of the scalar order parameter, but these aspects of the problem are expected to be important only if the analysis is supposed to yield quantitative rather than only qualitative results. We assume also that there is a periodic distribution of the surface easy direction, which is supposed to mimic an aligning surface obtained by applying any of the experimental techniques mentioned above.

Our paper is organized as follows. In Sec. II we present the model used for the theoretical investigations. The elastic and electrostatic problems are solved in the limit of small deviations from the homeotropic orientation within the NLC sample, taking into account dielectric properties of the substrates and considering a finite anchoring energy at the NLC-solid substrate interface. Apart from this most general case, in special cases of strong anchoring, contact with a conductive medium, or of a NLC without flexoelectric properties, analytical profiles for the director field and the electrical potential are derived. In Sec. III the theoretical results are critically discussed. It is also demonstrated that it is impossible to find a simple recipe to take into account the flexoelectric polarization.

II. MODEL

Consider a nematic slab of thickness $d=2D$, limited by two identical substrates, tending to orient NLC molecules parallel to the local surface normal. Due to specific surface treatment, let these substrates be characterized by a periodic

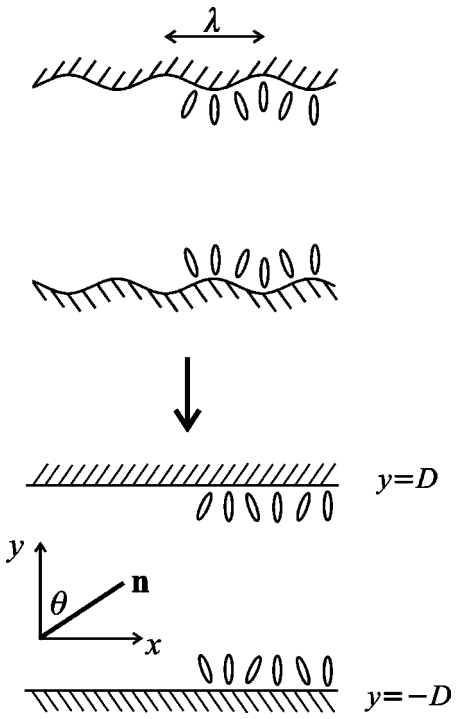

FIG. 1. Slab geometry: an undulating surface with locally homeotropic anchoring is replaced by a flat substrate with a modulated anchoring easy axis. The definition of the tilt angle θ and of the wavelength λ.

surface geometry. In the framework of our model, such substrates will be simulated by flat surfaces with an anchoring easy axis which varies periodically around the average, i.e., homeotropic orientation. Let us define a Cartesian reference frame with the origin in the middle of the slab. The limiting substrates are then located at $y=\pm D$ and the x axis is parallel to them (see Fig. 1). The system under consideration is formed by the lower (l) $\mathcal{R}_l$ ($y\leqslant -D$) and upper (u) $\mathcal{R}_u$ ($y\geqslant D$) regions outside the slab, representing the substrates, and the region $\mathcal{R}_n$ ($-D<y<D$) between them, representing the nematic liquid crystal (n). Our analysis will be limited to two-dimensional planar deformations, thereby assuming the twist distortion to be absent. In this framework the nematic director $\mathbf{n}=\mathbf{n}(x,y)$ is fully defined in terms of the tilt angle $\theta(x,y)$, as shown in Fig. 1: $\mathbf{n}=\mathbf{i}\sin\theta(x,y)+\mathbf{j}\cos\theta(x,y)$, where $\mathbf{i}$ and $\mathbf{j}$ are unit vectors parallel to the x and y axes, respectively. The flexoelectric polarization $\mathbf{P}$ is given by $\mathbf{P}=e_{11}\mathbf{n}\,\mathrm{div}\,\mathbf{n}-e_{33}\mathbf{n}\times\mathrm{rot}\,\mathbf{n}$. In such a planar and two-dimensional problem it is possible to rewrite $\mathbf{P}$ in terms of the tilt angle θ,

$$\mathbf{P}=\mathbf{i}\left[\frac{e}{2}\sin(2\theta)\frac{\partial\theta}{\partial x}-(e\sin^2\theta-e_{33})\frac{\partial\theta}{\partial y}\right]-\mathbf{j}\left[(e\sin^2\theta-e_{11})\frac{\partial\theta}{\partial x}+\frac{e}{2}\sin(2\theta)\frac{\partial\theta}{\partial y}\right], \tag{1}$$

where $e=e_{11}+e_{33}$. In the limit of $|\theta|\ll 1$ and $|\theta^2(\partial\theta/\partial y)|\ll|\theta(\partial\theta/\partial x)|\ll|\partial\theta/\partial y|$, $\mathbf{P}$ reduces to

$$\mathbf{P}=\mathbf{i}e_{33}\frac{\partial\theta}{\partial y}+\mathbf{j}e_{11}\frac{\partial\theta}{\partial x}. \tag{2}$$

Using $\mathbf{E}$ and θ as thermodynamical coordinates, the bulk thermodynamical potential density of the nematic liquid crystal is given by

$$f_n=\frac{1}{2}k(\nabla\theta)^2-\frac{1}{2}\epsilon E^2-\mathbf{P}\cdot\mathbf{E} \tag{3}$$

in the one elastic constant approximation and assuming an isotropic dielectric constant [1]. The total bulk thermodynamical potential densities of the substrates reduce to the electrostatic energy densities

$$f_l=-\frac{1}{2}\epsilon_s E_l^2 \quad\text{and}\quad f_u=-\frac{1}{2}\epsilon_s E_u^2, \tag{4}$$

where ϵ_s is the dielectric constant of the substrates, $E_l=E(x,y\leqslant -D)$, and $E_u=E(x,y\geqslant D)$.

The total thermodynamical potential of the NLC together with both substrates (per unit length along the z axis) is now given by

$$\mathcal{F}=\sum_m\int_{\mathcal{R}_m} f_m(x,y)\,dx\,dy+\mathcal{F}_s, \tag{5}$$

where $m=l$, n, and u. Here $\mathcal{F}_s$ is the anisotropic surface energy contribution which can be associated with the periodic surface topography of the NLC-substrate interface. To make our calculation as simple as possible, we represent an undulated surface whose periodicity is characterized by a wavelength $\lambda=2\pi/q$ (q denoting the corresponding wavevector) by a model plane surface with a sine-modulated anchoring easy axis $\theta(x)=\Theta_0\sin(qx)$ (see Fig. 1). The surface free energy of such an interface can then be written as

$$\mathcal{F}_s=\frac{1}{2}w[\theta(x,-D)+\Theta_0\sin(qx)]^2+\frac{1}{2}w[\theta(x,D)-\Theta_0\sin(qx)]^2, \tag{6}$$

where we assume that the anchoring strength w is the same on the two surfaces. Further, we choose a particular case where the easy axes are such as to impose antisymmetric orientations, hence the waves characterizing the anchoring of both substrates are in exact counterphase.

Since $\mathrm{rot}\,\mathbf{E}=0$, $\mathbf{E}=-\nabla\phi$, where ϕ is the electrical potential. By minimizing $\mathcal{F}$ given by Eq. (5) one obtains the bulk differential equations

$$\frac{\partial^2\phi_i}{\partial x^2}+\frac{\partial^2\phi_i}{\partial y^2}=0 \quad\text{for}\quad (x,y)\in\mathcal{R}_i, \tag{7}$$

where $i=l,u$, for the substrates, and

$$\frac{\partial^2\phi}{\partial x^2}+\frac{\partial^2\phi}{\partial y^2}-\frac{e}{\epsilon}\frac{\partial^2\theta}{\partial x\,\partial y}=0 \quad\text{for}\quad (x,y)\in\mathcal{R}_n, \tag{8}$$

for the electrical potential in the nematic liquid crystal. Further, the equation for the nematic tilt angle (obtained again by minimizing $\mathcal{F}$) reads

$$\frac{\partial^2\theta}{\partial x^2}+\frac{\partial^2\theta}{\partial y^2}+\frac{e}{k}\frac{\partial^2\phi}{\partial x\,\partial y}=0 \quad \text{for } (x,y)\in\mathcal{R}_n. \tag{9}$$

Equations (7)–(9) have to be solved in agreement with the boundary conditions

$$\left[-\epsilon_s\frac{\partial\phi_i}{\partial y}\right]_{y=\pm D}=\left[-\epsilon\frac{\partial\phi}{\partial y}+e_{11}\frac{\partial\theta}{\partial x}\right]_{y=\pm D}, \tag{10}$$

$$\phi_i(\pm D)=\phi(\pm D), \tag{11}$$

and

$$\pm\left[k\frac{\partial\theta}{\partial y}+e_{33}\frac{\partial\phi}{\partial x}\right]_{y=\pm D}+w[\,\theta(x,\pm D)\mp\Theta_0\sin(qx)\,]=0. \tag{12}$$

Here Eqs. (10) and (11) represent the continuity of the normal component of the dielectric displacement and of ϕ at the interfaces $y=\pm D$, respectively, while Eqs. (12) represent the balance of the bulk and surface torques.

The symmetry of the electrical problem and the antisymmetrical boundary conditions for θ lead to the following properties:

$$\theta(x,y)=-\theta(x,-y) \quad \text{and} \quad \phi(x,y)=\phi(x,-y). \tag{13}$$

The solutions of linear differential equations (7)–(9), satisfying the boundary conditions (10)–(12) and the symmetry condition (13), can be written as

$$\phi_i(x,y)=\beta e^{\pm qy}\cos(qx), \tag{14}$$

where $+$ corresponds to $i=l$ and $-$ to $i=u$, which gives the electrical potential in the substrates; further,

$$\phi(x,y)=[\,\mu_1\cosh(\alpha_1 y)+\mu_2\cosh(\alpha_2 y)]\cos(qx) \tag{15}$$

gives the electrical potential in the nematic layer, and, finally,

$$\theta(x,y)=R[\,\mu_1\sinh(\alpha_1 y)+\mu_2\sinh(\alpha_2 y)]\sin(qx) \tag{16}$$

is the solution for the nematic tilt angle profile. The intrinsic flexoelectric lengths α_1^{-1} and $|\alpha_2|^{-1}$ and the quantity R are given by

$$\alpha_{1,2}=q(s\pm\sqrt{s^2+1}), \quad R=\sqrt{\epsilon/k}, \quad \text{where } s=\sqrt{e^2/4\epsilon k}. \tag{17}$$

The parameter s is proportional to $e=e_{11}+e_{33}$ and thus takes into account flexoelectric properties of the liquid crystal. The constants β, μ_1, and μ_2 depend on the flexoelectric coefficients e_{11} and e_{33}, on the dielectric constant of the substrates, ϵ_s, and on the ratio of the elastic constant versus the anchoring strength, denoted by the extrapolation length $L_e=k/w$. (They also depend on the material constants k and ϵ, which be treated as fixed.) Their forms follow from the boundary conditions (10)–(12) and are given by

$$\beta(e_{11},e_{33};L_e,\epsilon_s)=\frac{\beta(e_{11},e_{33};0,\epsilon_s)}{\Omega(e_{11},e_{33};L_e,\epsilon_s)}$$

$$\text{and} \quad \mu_{1,2}(e_{11},e_{33};L_e,\epsilon_s)=\frac{\mu_{1,2}(e_{11},e_{33};0,\epsilon_s)}{\Omega(e_{11},e_{33};L_e,\epsilon_s)}, \tag{18}$$

where $\beta(e_{11},e_{33};0,\epsilon_s)$ and $\mu_{1,2}(e_{11},e_{33};0,\epsilon_s)$ are the constants obtained in the strong anchoring regime, where $w\to\infty$ and, consequently, $L_e=0$. Further, $\Omega(e_{11},e_{33};L_e,\epsilon_s)$ is defined by

$$\Omega(e_{11},e_{33};L_e,\epsilon_s)=1+L_e\left\{\frac{C_2\left(\alpha_1-\frac{qe_{33}}{Rk}\right)\tanh(\alpha_2 D)-C_1\left(\alpha_2-\frac{qe_{33}}{Rk}\right)\tanh(\alpha_1 D)+\alpha_2-\alpha_1}{\tanh(\alpha_2 D)-\tanh(\alpha_1 D)+(C_2-C_1)\tanh(\alpha_1 D)\tanh(\alpha_2 D)}\right\}, \tag{19}$$

where $C_{1,2}=(qe_{11}R-\alpha_{1,2}\epsilon)/(q\epsilon_s)$. Furthermore,

$$\beta(e_{11},e_{33};0,\epsilon_s)=e^{qD}\sum_{i=1}^{2}\mu_i(e_{11},e_{33};0,\epsilon_s)\cosh(\alpha_i D) \tag{20}$$

and

$$\mu_{1,2}(e_{11},e_{33};0,\epsilon_s)=\frac{\mu_{1,2}(e_{11},e_{33};0,\infty)}{M_{1,2}(e_{11},e_{33};0,\epsilon_s)}, \tag{21}$$

where

$$M_{1,2}(e_{11},e_{33};0,\epsilon_s)=\frac{1+(C_2-C_1)\dfrac{\sinh(\alpha_1 D)\sinh(\alpha_2 D)}{\sinh[(\alpha_2-\alpha_1)D]}}{1-C_{2,1}\tanh(\alpha_{2,1}D)} \tag{22}$$

and

$$\mu_{1,2}(e_{11},e_{33};0,\infty)=\mp\frac{\Theta_0}{R}\frac{\cosh(\alpha_{2,1}D)}{\sinh[(\alpha_2-\alpha_1)D]} \tag{23}$$

correspond to a NLC in contact with a conductive surface (for which $\epsilon_s\to\infty$) in the strong anchoring limit. The relations reported above give the general solution of the problem. In the following some particular cases will be considered.

A. Nonflexoelectric materials

First we consider the nonflexoelectric nematic material ($e_{11}=e_{33}=0$). This implies that $s=0$, $\alpha_1=-\alpha_2=q$, and $C_{1,2}=\mp(\epsilon/\epsilon_s)$. Consequently,

$$\Omega(0,0;L_e,\epsilon_s)=1+qL_e\coth(qD), \tag{24}$$

and, according to Eqs. (20)–(23), $\beta(0,0;0,\epsilon_s)=0$, $M_{1,2}(0,0;0,\epsilon_s)=1$, and

$$\mu_{1,2}(0,0;0,\epsilon_s)=\mu_{1,2}(0,0;0,\infty)=\pm\frac{\Theta_0}{R}\frac{1}{2\sinh(qD)}. \tag{25}$$

From Eqs. (14) and (15) it follows that for $e_{11}=e_{33}=0$ the electrical potential $\phi(x,y)=0$ everywhere, and from Eq. (16)

$$\theta(x,y)=\Theta_0\frac{\sinh(qy)}{\sinh(qD)}\left[\frac{1}{1+qL_e\coth(qD)}\right]\sin(qx) \overset{L_e\to 0}{\to} \Theta_0\frac{\sinh(qy)}{\sinh(qD)}\sin(qx). \tag{26}$$

The last expression describes the tilt angle profile in the strong anchoring limit.

B. Nematic liquid crystal in contact with a conductive medium

In this case $\epsilon_s\to\infty$, hence $C_{1,2}\to 0$. Consequently, from Eq. (19) $\Omega(e_{11},e_{33};L_e,\infty)$ is found to be

$$\Omega(e_{11},e_{33};L_e,\infty)=1+L_e\frac{\alpha_2-\alpha_1}{\sinh[(\alpha_2-\alpha_1)D]}\times\cosh(\alpha_1 D)\cosh(\alpha_2 D), \tag{27}$$

and, according to Eqs. (20)–(23), $M_{1,2}(e_{11},e_{33};0,\infty)=1$ and $\beta(e_{11},e_{33};0,\infty)=0$. In this framework, using Eqs. (18), we also have $\beta(e_{11},e_{33};L_e,\infty)=0$. As expected, the electrical potential in the substrates vanishes. Moreover,

$$\mu_{1,2}(e_{11},e_{33};L_e,\infty)=\mp\frac{\Theta_0}{R}\frac{\cosh(\alpha_{2,1}D)}{\sinh[(\alpha_2-\alpha_1)D]+L_e(\alpha_2-\alpha_1)\cosh(\alpha_1 D)\cosh(\alpha_2 D)}. \tag{28}$$

The tilt angle $\theta(x,y)$ and the electrical potential $\phi(x,y)$ can be obtained easily by substituting Eqs. (28) into Eqs. (15) and (16). Simple calculations give

$$\theta(x,y)=\Theta_0\frac{-\cosh(\alpha_2 D)\sinh(\alpha_1 y)+\cosh(\alpha_1 D)\sinh(\alpha_2 y)}{\sinh[(\alpha_2-\alpha_1)D]+L_e(\alpha_2-\alpha_1)\cosh(\alpha_1 D)\cosh(\alpha_2 D)}\sin(qx) \tag{29}$$

and

$$\phi(x,y)=\frac{1}{R}\Theta_0\frac{-\cosh(\alpha_2 D)\cosh(\alpha_1 y)+\cosh(\alpha_1 D)\cosh(\alpha_2 y)}{\sinh[(\alpha_2-\alpha_1)D]+L_e(\alpha_2-\alpha_1)\cosh(\alpha_1 D)\cosh(\alpha_2 D)}\cos(qx). \tag{30}$$

Again, in the strong anchoring regime the formulas for $\theta(x,y)$ and $\phi(x,y)$ can be derived simply by substituting $L_e=0$ into Eqs. (29) and (30).

III. RESULTS AND DISCUSSION

In the preceding section, we have derived analytical formulas for the tilt angle profile $\theta(x,y)$ and the electrical potential $\phi(x,y)$, assuming the tilt angle to be small. Now we are going to analyze the physical behavior of these solutions for different values of the flexoelectric coefficient $e=e_{11}+e_{33}$ and surface periodicity wave vector q. Moreover, we would like to relate $\theta(x,y)$ profiles to a quantity that can be detected experimentally. An appropriate choice turns out to be $\langle\theta^2\rangle$, i.e., the square of the tilt angle θ averaged over the nematic slab

$$\langle\theta^2\rangle=\frac{1}{2\lambda D}\int_{-D}^{D}\int_{-\lambda/2}^{\lambda/2}\theta^2(x,y)\,dx\,dy, \tag{31}$$

where $\lambda=2\pi/q$. The quantity $\langle\theta^2\rangle$ can be detected, for example, in a dielectric measurement or in a measurement of the optical path difference [13]. In addition, we have also investigated elastic and electrostatic contributions to the thermodynamical potential density in order to obtain some insight into the mechanisms which determine the director profile.

A. Characteristic lengths

Both $\theta(x,y)$ and $\phi(x,y)$ profiles are periodic in x and can be written, according to Eqs. (15) and (16), as $\theta(x,y)=t(y)\sin(qx)$ and $\phi(x,y)=f(y)\cos(qx)$. For simplicity, in the following we plot only y-dependent parts of the profiles, namely the ''amplitudes'' $t(y)$ and $f(y)$. As it can be deduced from Eqs. (15) and (16), these are characterized by two characteristic lengths $1/\alpha_1$ and $1/|\alpha_2|$, both depending on the dimensionless parameter s and hence being related to the flexoelectric coefficient e and on periodicity q [see Eqs. (17)]. Note that when the flexoelectricity is absent ($s\to 0$), $\alpha_1=|\alpha_2|=q$, i.e., both lengths become equal, while for pronounced flexoelectricity (s large) one of them decreases ($1/\alpha_1\to 1/2qs$), while the other one increases ($1/|\alpha_2|\to\infty$ for $s\to\infty$). Hence, for fixed q and large enough s in the nematic sample there are two well distinguished areas with characteristic behaviors of the profiles, one of these areas being localized to a subsurface layer, and the other spreading through the rest of the sample. For small s it is impossible to distin-

guish between the short and long scale contributions since $\alpha_1 \sim |\alpha_2| \sim q$. On the other hand, keeping s fixed (and nonzero) and increasing the value of q, both characteristic lengths decrease. Note that also in this case the distinction between the long and short scale contributions is enhanced with increasing q. One can conclude that a kind of subsurface deformation appears in the vicinity of the substrate. Increasing both s and q, this deformation becomes more and more localized. Such qualitative behavior applies to solutions obtained for all types of elastic and electrostatic boundary conditions considered in the analysis. The boundary conditions themselves merely determine the actual surface values of the tilt angle and of the electrical potential, but do not alter any qualitative features of bulk solutions.

In order to understand the source of such behavior, it is convenient to reconsider the bulk part of the thermodynamical potential density (3). Since the x dependence of θ and ϕ profiles is known to be given by $\sin(qx)$ and $\cos(qx)$, respectively, the thermodynamical potential density $f_n(x,y)$ can be integrated over x, yielding

$$\tilde{f}_n(y) \propto (q^2 t^2 + t'^2) - R^2(q^2 f^2 + f'^2) + 2Rsq(tf' - t'f), \tag{32}$$

where $t' = dt/dy$ and $f' = df/dy$. Further, $e_{11} = e_{33} = e/2$ was assumed. The expression (32) consists of elastic, homogeneous electrostatic, and flexoelectric contributions. The third term couples elastic and electrostatic variables. Considering first the $s = 0$ case where the flexoelectricity is absent, only the first, i.e., the elastic term is relevant. Dealing with homogeneous anchoring ($q = 0$), the tilt angle profile $t(y)$ minimizing the thermodynamical potential is described by a linear function, as predicted by the ordinary Frank elastic theory for a NLC between two plane-parallel plates. For $q \neq 0$, however, the bulk tends towards the homeotropic alignment with $t = 0$ in order to minimize the positive $q^2 t^2$ contribution in Eq. (32), thereby producing a sort of subsurface deformation if the amplitude of the boundary tilt angle, Θ_0, is different from 0. Hence, with increasing q the subsurface deformation becomes increasingly localized. This conclusion could be made also by simply plotting the director field in the vicinity of the modulated substrate imposing a molecular alignment parallel to the local surface normal.

Let us now consider the $s \neq 0$ case, where the flexoelectricity is present. For clarity, we rewrite the flexoelectric contribution [last term in Eq. (32)] as $2Rsq(tf' - t'f) = 2Rsq[t^2 d(f/t)/dy]$. Equation (32) can now be rewritten as

$$\tilde{f}_n(y) \propto t'^2 + t^2 \left[q^2 + 2Rsq \frac{d(f/t)}{dy} \right] - R^2(q^2 f^2 + f'^2). \tag{33}$$

The function $d(f/t)/dy$ appearing, beside the q^2 term, in the proportionality constant of t^2, turns out to be a positive function (for $S > 0$), strongly peaked in the middle of the sample at $y = 0$ [where $t(y)$ itself is equal to zero], while approaching a nonzero but small value elsewhere. It also turns out that the dependences t^2 and $t^2 d(f/t)/dy$ are qualitatively similar and hence it can be reasonable to approximate the proportionality constant of t^2 as $q^2 + 2Rsq[d(f/t)/dy] \sim Q(s,q)$, where $Q(s,q)$ is a positive and monotonically increasing function of both $|s|$ and q. Using now the same reasoning as above for the $s = 0$ case, it can be deduced that through increasing not only q but also $|s|$, the subsurface deformation becomes increasingly localized. The former increase arises from the elastic free energy while the origin of the latter is the flexoelectric contribution.

B. Profiles and observables

In the following we will again suppose $e_{11} = e_{33} = e/2$ in order to reduce the parameter space, which is expected not to change any of the main conclusions of the present analysis. We have expressed the flexoelectric coefficient e in terms of the dimensionless quantity s (17). Setting $e = 8.8 \times 10^{-11}$ As/m, as measured for MBBA in Ref. [13], and, further, $k = 5 \times 10^{-12}$ N and $\epsilon \sim 5\epsilon_0$ [1], yields $s \sim 3$. Therefore, in our analysis we will consider the range $0 < s \lesssim 3$, where the $s = 0$ limit corresponds to the absence of flexoelectricity in the material. Further, we choose $q = 1/D$ and $q = 3/D$. Note that in Eq. (2) giving the flexoelectric polarization, we have performed an expansion for small $|\theta|$ and for $|\theta^2(\partial\theta/\partial y)| \ll |\theta(\partial\theta/\partial x)| \ll |\partial\theta/\partial y|$ Although in our case ($\Theta \sim 5°$) this condition is already slightly violated, we decided not to reduce the value of Θ_0 any further because this would not correspond to a real modulated substrate used for technological purposes. This inconsistency is, however, not expected to influence the qualitative behavior of our results. Finally, we choose $D \sim 1$ μm. Note that although here for $q = 3/D$ the periodicity λ amounts to ~ 2 μm, the characteristic distortion length $1/\alpha_1$ for sufficiently high values of s is in the submicron range.

Let us first analyze the θ profiles in a strongly anchored nematic liquid crystal in contact with conductive substrates (Fig. 2), a case which is rather simple as far as mechanical and electrical boundary conditions are concerned. As the surface gratings are supposed to be in exact counterphase, $t(\pm D) = \pm\Theta_0$, which in our case was set to $\Theta_0 = 5°$. For large enough values of s and q, the $t(y)$ profile indeed represents a kind of subsurface deformation, which is for, e.g., $s = 3$ and $q = 3/D$ (the largest values of s and q considered) limited to a layer of thickness $\sim 0.1D = 100$ nm. In that case the molecular orientation in the bulk approaches the homeotropic alignment while in the absence of flexoelectricity ($s = 0$) the subsurface deformation is less pronounced and the bulk tendency to approach homeotropic alignment is weaker. Consequently, for large s and q the observable quantity $\langle \theta^2 \rangle$ will be smaller than the one obtained for small values of s and q. From Fig. 5(a) it is evident that in fact $\langle \theta^2 \rangle$ is a monotonically decreasing function of both s and q.

Let us now consider tilt angle profiles for weak anchoring, still retaining the conductive substrates. Figure 3 presents $t(y)$ profiles calculated for $L_e = 100$ nm [31]. As expected, for a finite anchoring strength the amplitude of the subsurface deformation is reduced, if compared to the infinite anchoring case. Consequently, also the resulting values of $\langle \theta^2 \rangle$ are fairly lower. However, note that the qualitative behavior of $\langle \theta^2 \rangle$ versus s [Fig. 5(a)] is still the same as in the infinite anchoring limit.

Finally, let us analyze a more general case, where the substrates confining the nematic liquid crystal are not con-

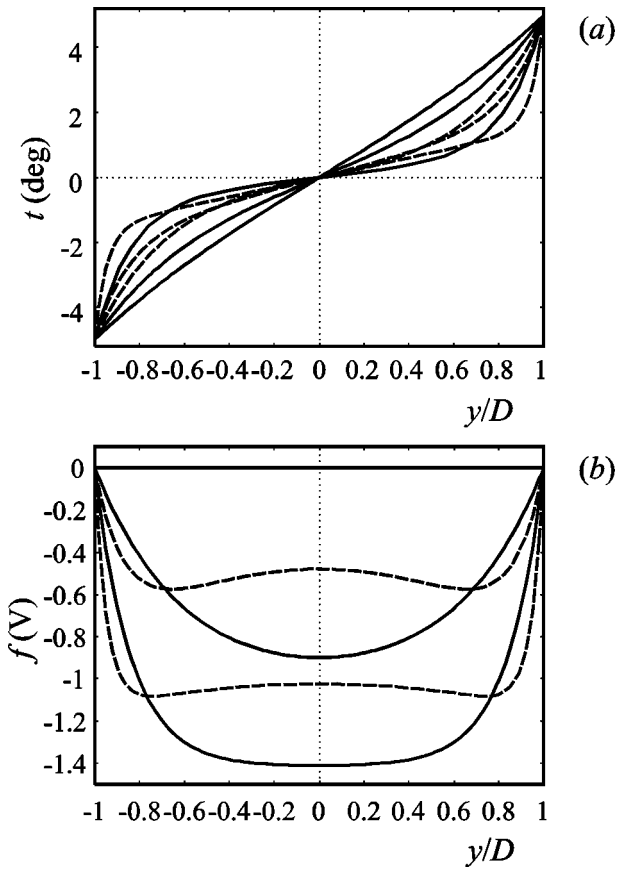

FIG. 2. Strongly anchored NLC ($L_e=0$) and conductive substrates ($\epsilon/\epsilon_s=0$). Solid curves correspond to $q=1/D$, while the dashed curves correspond to $q=3/D$; $\Theta_0=5°$ and $D=1$ μm. (a) Director profiles $t(y)$: within each set of curves (solid or dashed) the one with the highest slope at $y=0$ corresponds to $s=0$, the one with the lowest slope to $s=3$, while the one in between them corresponds to $s=1$. (b) Electrical potential profiles $f(y)$: the top (straight) curve corresponds to $s=0$, the bottom one to $s=3$, and the one in between to $s=1$ (again within the solid and the dashed sets, respectively).

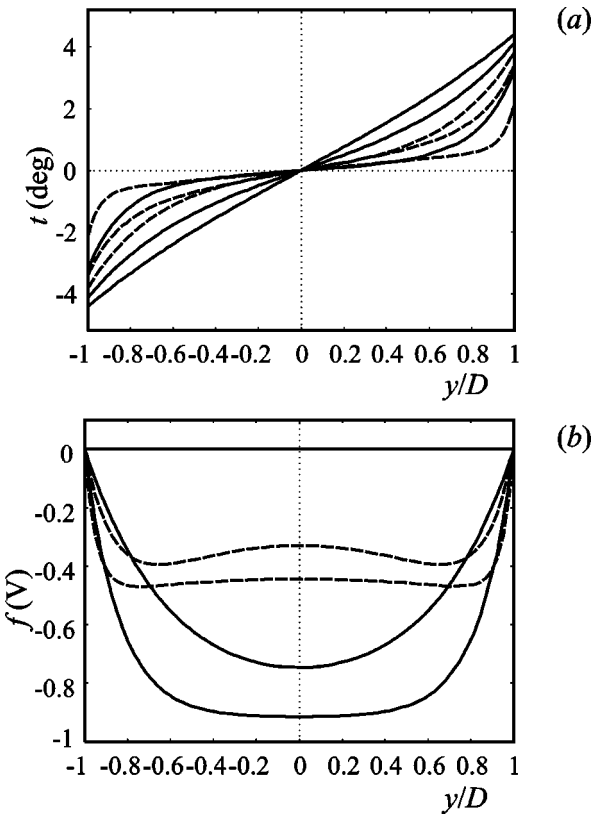

FIG. 3. Weak anchoring ($L_e=0.1D$) and conductive substrates ($\epsilon/\epsilon_s=0$): (a) $t(y)$ profiles, (b) $f(y)$ profiles. Other parameters and conventions are the same as those given in the caption of Fig. 2.

ductive plates but, rather, consist of a dielectric material characterized by a finite dielectric constant. Further, let us again assume the weak anchoring condition at the confining boundaries. Looking at Figs. 4 and 5(a), it is possible to deduce that both the tilt angle profiles and the $\langle\theta^2\rangle$ versus s dependence are almost identical to those obtained for the conductive substrates and that the orientational ordering within the nematic slab is almost insensitive to the changes of ϵ_s, the dielectric permittivity of the substrates.

We have also plotted the y dependences of the electrical potential in the nematic cell [$f(y)$, Figs. 2(b), 3(b), and 4(b)]. Their qualitative features do not change considerably with changing boundary conditions. Dealing with conductive substrates, the surface value of the potential is fixed (e.g., to 0), while if dealing with dielectric ones the potential is fixed only at $y=\pm\infty$, but not at the interfaces where it can vary. Also the $f(y)$ profiles show a variation localized close to substrates (again for large enough s and q), while the variations in the bulk are rather smooth. The $f(y)$ profiles are not very interesting for our analysis since they are not directly connected to the observable $\langle\theta^2\rangle$.

In Sec. II we have determined the electrical potential and the tilt angle fields, $\phi(x,y)$ and $\theta(x,y)$, respectively. Using the solutions $\phi(x,y)$ and $\theta(x,y)$, it is possible to evaluate the electrostatic ($f_E=-\frac{1}{2}\epsilon E^2-\mathbf{P}\cdot\mathbf{E}$), Frank elastic [$f_F=\frac{1}{2}k(\nabla\theta)^2$], and the total bulk nematic ($f_n=f_F+f_E$) contributions to the thermodynamical potential. We have plotted f_n as a function of x and y (Fig. 6), and for large enough s and q both f_F and f_E turn out to be localized in a subsurface layer. Further, our results show that the elastic and electrostatic contributions to the thermodynamical potential are comparable, except for $s\to 0$, when $f_E\ll f_F$. This proves that if the characteristic deformation scale is small with respect to the Debye screening length, f_E cannot be neglected when $\phi(x,y)$ and $\theta(x,y)$ are determined. In fact, it has been well known already for a long time [14] that a correct description of piezoelectric materials, which in some aspects are similar to flexoelectric nematics, implies solving two types of differential equations: those following from the mechanical equilibrium, and the Maxwell equations $\mathrm{div}\,\mathbf{D}=0$, $\mathrm{rot}\,\mathbf{E}=0$, with the constitutive equation $\mathbf{D}=\epsilon\mathbf{E}+\mathbf{P}$.

C. Anchoring versus flexoelectricity

As already mentioned, in the weak anchoring case, the value of the observable $\langle\theta^2\rangle$ for given q and s is lower (for $L_e\sim 100$ nm roughly by 20% if $q=1/D$ and by 40% if $q=3/D$) from the value obtained in the strong anchoring limit (Fig. 5). On the other hand, $\langle\theta^2\rangle$ decreases with increasing s, too. Plotting $\langle\theta^2\rangle$ as a function of the extrapolation length L_e and ignoring flexoelectricity [$s=0$, Fig. 5(b)], we observe

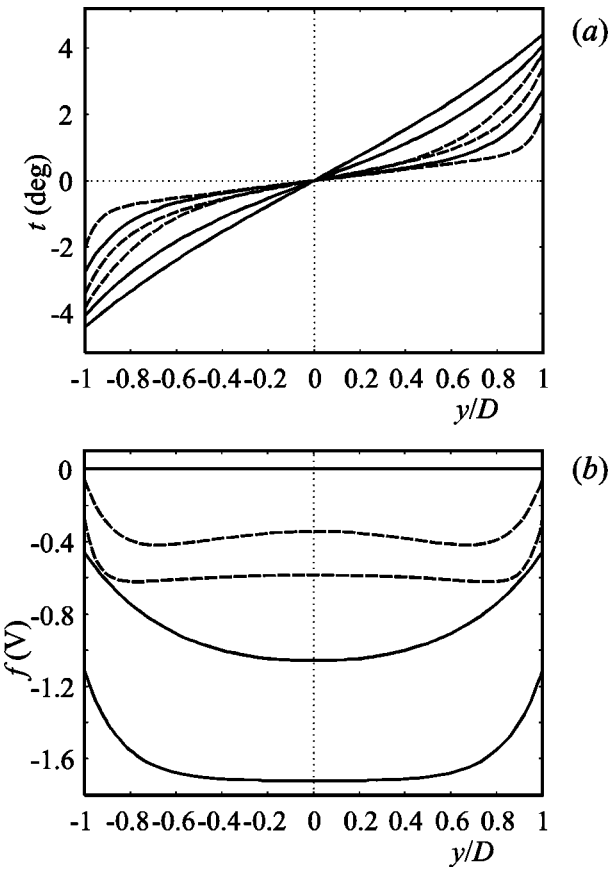

FIG. 4. Weak anchoring ($L_e=0.1D$) and conductive substrates ($\epsilon/\epsilon_s=1$, $R=3/V$): (a) $t(y)$ profiles, (b) $f(y)$ profiles. Other parameters and conventions are the same as those for Fig. 2.

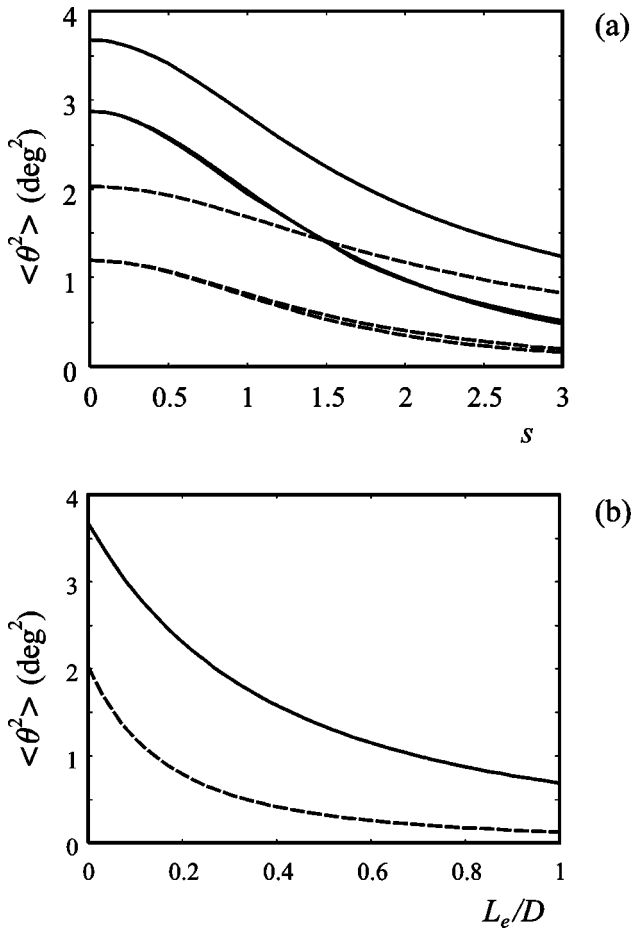

FIG. 5. (a) Observable $\langle\theta^2\rangle$ vs s for different q: solid lines, $q=1/D$; dashed lines, $q=3/D$. Within each set of curves, the top one corresponds to strong anchoring and conductive substrates, the bottom one to weak anchoring and conductive substrates, while the one in between to weak anchoring and dielectric substrates (the last two being almost indistinguishable). All other parameters are the same as in the corresponding cases shown in Figs. 2, 3, and 4. (b) $\langle\theta^2\rangle$ vs L_e in the absence of flexoelectricity; the solid line corresponds to $q=1/D$, and the dashed line to $q=3/D$.

that $\langle\theta^2\rangle$ is a monotonically decreasing function of L_e as well, exhibiting a behavior similar to that of the $\langle\theta^2\rangle$ versus s dependence. Therefore, measuring only the value of $\langle\theta^2\rangle$, it is impossible to conclude which mechanism is responsible for its decrease. According to the above considerations, a possible conclusion could be that there is a correspondence between a finite anchoring strength and a nonzero flexoelectric coefficient, i.e., that flexoelectricity in our problem just renormalizes the anchoring strength w. But, trying to compare actual tilt angle profiles (Fig. 7) for $s=0$ and $s\neq 0$ and then adjusting the corresponding anchoring strengths so as to obtain the same value of $\langle\theta^2\rangle$, it is evident that an exact one-to-one mapping between the effective anchoring strength and the flexoelectric coefficient does not exist. In fact, for $s=0$ both characteristic lengths discussed above become equal to q, while for a nonzero s they differ essentially (the shorter one being related to the subsurface deformation). This implies a substantial disagreement of the actual $t(y)$ profiles in the nematic bulk, although the average values $\langle\theta^2\rangle$ may be the same. It is, therefore, impossible to state that the effect of flexoelectricity is just to renormalize w, although the result for w strongly depends on whether flexoelectricity has been taken into account or not.

However, by measuring the temperature (T) dependence of $\langle\theta^2\rangle$, it could be possible to gain some information concerning the interplay of flexoelectricity and weak anchoring, which drive the behavior of $t(y)$ profiles and, consequently, of $\langle\theta^2\rangle$. Recall that $\langle\theta^2\rangle$ is a monotonically decreasing function of s (for fixed L_e and q), or of L_e (for fixed s and q). Expressing s in terms of the nematic scalar order parameter S and assuming $k\propto S^2$ [1] and $e\propto aS+bS^2$ [5] yields $s\propto a+bS$. The relative magnitude of the constants a and b depends on the microscopic origin of flexoelectricity: $a\gg b$ for quadrupolar flexoelectricity and vice versa for dipolar flexoelectricity [4,32]. Therefore, in the former case the value of s is expected not to be very sensitive to changing S (in this case $s\propto a\sim$ const), while in the latter it is rather the opposite (then $s\propto bS\neq$ const [32]). Expressing further $L_e=k/w$ results in $L_e\propto S$, where $w\propto S$ has been assumed [33]. Consequently, if we are dealing with the dipolar flexoelectricity, the L_e versus S and s versus S dependences are indistinguishable. If, however, the flexoelectricity is of quadrupolar origin, the two effects can be distinguished since in this case s is essentially S-independent while $L_e\propto S$ still holds. Increasing the temperature, S decreases and then, consequently, L_e decreases, while s remains almost unchanged. Hence, if flexoelectricity is of quadrupolar origin and the anchoring is strong, $\langle\theta^2\rangle$ should be almost insensitive to changes of T. If, on the contrary, flexoelectricity is of dipolar origin or the

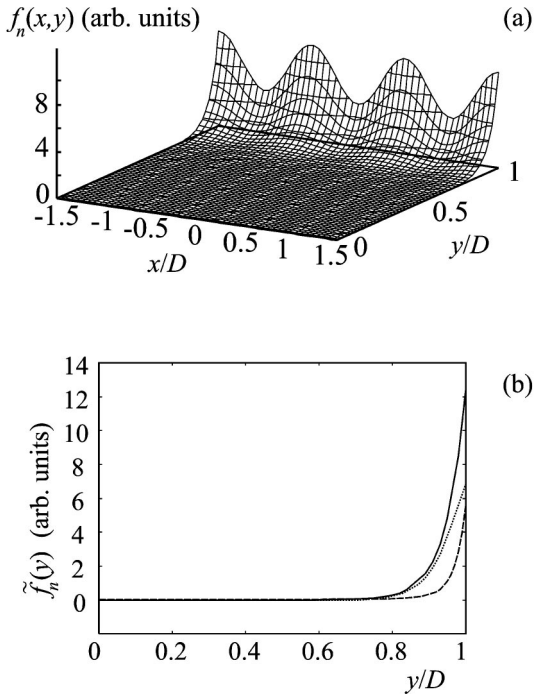

FIG. 6. NLC in contact with dielectric substrates. (a) The total bulk thermodynamical potential density $f_n(x,y)$. (b) $\tilde{f}_n(y) = \int f_n(x,y)dx$ (solid line), the Frank elastic contribution to $\tilde{f}_n(y)$ (dashed line), and the electrostatic contribution to $\tilde{f}_n(y)$ (dotted line). $s=3$ and $q=3/D$, while all other parameters are the same as those given in the captions of Figs. 2 and 4.

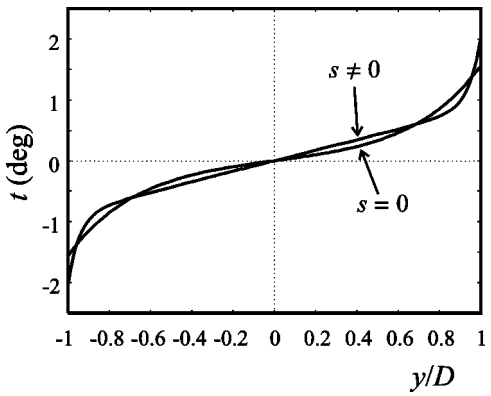

FIG. 7. Comparison of two director profiles $t(y)$ in a weakly anchored NLC in contact with dielectric substrates with $(s\neq 0)$ and without flexoelectricity $(s=0)$; $q=3/D$. The anchoring strength has been adjusted so as to obtain the same value of $\langle\theta^2\rangle$ in both cases: for $s=3$, $L_e=0.1D$, while for $s=0$, $L_e\sim 0.73D$. Note the different characteristic lengths of the subsurface deformation. $\epsilon/\epsilon_s = 1$, $R=3/V$.

anchoring is weak, $\langle\theta^2\rangle$ is expected to increase when heating the sample.

IV. CONCLUSION

In the present analysis we have considered elastic deformations in a flexoelectric nematic material, occurring close to the nematic-substrate interface due to the periodic surface topography of the substrate. We focused our attention on cases where the surface periodicity is high enough that the deformations occur on a submicrometric length scale well below the Debye screening length. In such cases the equilibrium director profile cannot be determined correctly if flexoelectricity is ignored. Therefore, we have performed a thorough analysis of elastic deformations in a nematic sample sandwiched between two parallel substrates, investigating this aspect of the problem. In order to establish a connection to experimental observables, we have calculated the average $\langle\theta^2\rangle$ and investigated its behavior.

Increasing either the periodicity of the surface gratings or the flexoelectric coefficient, a kind of subsurface deformation appears in the vicinity of the substrates. As an example, we show that if an experimental technique sensitive to $\langle\theta^2\rangle$ were employed to measure the anchoring strength, the results should be interpreted with extreme caution since they can depend substantially on the value of the flexoelectric coefficient. In fact, there is no simple procedure to describe flexoelectricity with an effective anchoring strength.

Neglecting flexoelectricity and the corresponding contribution to the thermodynamical potential can only be correct when in a specific NLC long-range electrostatic interactions are rather unimportant in comparison to the short-range ones, or when the elastic deformations in a flexoelectric material occur on length scales considerably larger than the Debye screening length. Although NLCs normally have pronounced flexoelectric properties, electrostatic interactions have often been neglected. This is probably correct for treating systems similar to the classical nematic cell used for many technological applications, but it is certainly wrong when the anchoring modulation occurs on a scale below the Debye screening length. In this respect our analysis is relevant for any study of microconfined NLC systems, such as microdroplets and microtubes.

In particular, we conclude that the analyses dealing with surfaces characterized by submicrometric inhomogeneous anchoring presented in [1,17–21] should be reconsidered taking into account effects of flexoelectricity. Although for our model surface the deviations from the homeotropic orientation in the effective anchoring easy axis are rather small and thus do not give rise to bistable ordering, our results indicate that flexoelectricity should be taken into account in analyses of real bistable surfaces. For example, the first-order phase transition between two orientational states with the bulk director in two perpendicular directions, predicted in Refs. [26,27], could be modified. Similarly, taking into account electrostatic effects could also affect the transition between the low and high pretilt regimes observed in Ref. [16]. Finally, analyses [24–28] dealing with the variation of the nematic scalar order parameter should, apart from including flexoelectricity, take into account order electric effects as well.

ACKNOWLEDGMENTS

We wish to acknowledge the financial support of the Ministry of Science and Technology of Slovenia (Grant No. J1-0595-1554-98), and of the European Union (Project INCO Copernicus No. ERBCIC15CT960744 and TMR network FMRX-CT 98-029).

[1] P. G. de Gennes and J. Prost, *The Physics of Liquid Crystals* (Clarendon Press, Oxford, 1993).
[2] R. B. Meyer, Phys. Rev. Lett. **22**, 918 (1969).
[3] C. Kittel, *Introduction to Solid State Physics* (Wiley, New York, 1953).
[4] J. Prost and J. P. Marcerou, J. Phys. (Paris) **38**, 315 (1977).
[5] A. L. Alexe-Ionescu, Phys. Lett. A **180**, 456 (1993).
[6] G. Barbero, I. Dozov, J. F. Palierne, and G. Durand, Phys. Rev. Lett. **56**, 2056 (1986).
[7] W. Helfrich, Mol. Cryst. Liq. Cryst. **26**, 1 (1974).
[8] H. J. Deuling, in *Solid State Physics*, Suppl. 14, edited by L. Liebert (Academic Press, New York, 1978).
[9] I. Dozov, G. Barbero, J. F. Palierne, and G. Durand, Europhys. Lett. **1**, 563 (1986).
[10] G. Barbero and G. Durand, J. Phys. (Paris) **47**, 2129 (1986).
[11] A. Rapini and M. Papoular, J. Phys. (Paris), Colloq. **30**, C4-54 (1969).
[12] R. N. Thurston, J. Cheng, R. B. Meyer, and G. D. Boyd, J. Appl. Phys. **56**, 263 (1984).
[13] N. V. Madhusudana and G. Durand, J. Phys. (France) Lett. **46**, L195 (1985).
[14] L. D. Landau and E. M. Lifshitz, *Electrodynamics of Continuous Media* (MIR, Moscow, 1974).
[15] M. Monkade, M. Boix, and G. Durand, Europhys. Lett. **5**, 697 (1988).
[16] G. P. Bryan-Brown, M. J. Towler, M. S. Bancroft, and D. G. Mc Donnell, in *Proceedings of the 1994 International Display Research Conference and International Workshops on Active-Matrix LCD's and Display Materials* (The Society for Information Display, Santa Ana, 1994), p. 209.
[17] D. W. Berreman, Phys. Rev. Lett. **28**, 1683 (1972).
[18] G. Barbero, T. Beica, A. L. Alexe-Ionescu, and R. Moldovan, J. Phys. II **2**, 2011 (1992).
[19] C. V. Brown, G. P. Bryan-Brown, and V. C. Hui, Mol. Cryst. Liq. Cryst. **301**, 163 (1997).
[20] C. Ferrero, V. Mocella, M. Sanchez del Rio, and R. Barberi, Mol. Mater. **9**, 109 (1997).
[21] R. Barberi, I. Dozov, M. Giocondo, M. Iovane, Ph. Martinot-Lagarde, D. Stoenescu, S. Tonchev, and L. V. Tsonev, Europhys. J. B **6**, 83 (1998).
[22] G. Barbero and G. Durand, J. Appl. Phys. **68**, 5549 (1990).
[23] A. L. Alexe Ionescu, Nuovo Cimento D **15**, 1489 (1993).
[24] G. Skačej, A. L. Alexe-Ionescu, G. Barbero, and S. Žumer, Phys. Rev. E **57**, 1780 (1998).
[25] M. C. J. M. Vissenberg, S. Stallinga, and G. Vertogen, Phys. Rev. E **55**, 4367 (1997).
[26] T. Z. Qian and P. Sheng, Phys. Rev. Lett. **77**, 4564 (1996).
[27] T. Z. Qian and P. Sheng, Phys. Rev. E **55**, 7111 (1997).
[28] V. Mocella, C. Ferrero, M. Iovane, and R. Barberi, Liq. Cryst. (to be published).
[29] P. Chiarelli, S. Faetti, and L. Fronzoni, J. Phys. (Paris) **44**, 1061 (1983).
[30] M. A. Osipov and T. J. Sluckin, J. Phys. II **3**, 793 (1993).
[31] L. M. Blinov, A. Yu. Kabayenkov, and A. A. Sonin, Liq. Cryst. **5**, 645 (1989).
[32] J. P. Marcerou and J. Prost, Mol. Cryst. Liq. Cryst. **58**, 259 (1980).
[33] M. Nobili and G. Durand, Phys. Rev. A **46**, R6174 (1992).